Research Article

Teresa Darlen Carrillo-Castillo, Antonia Luna-Velasco*,
Erasto Armando Zaragoza-Contreras*, and Javier Servando Castro-Carmona

Thermosensitive hydrogel for *in situ*-controlled methotrexate delivery

https://doi.org/10.1515/epoly-2021-0085
received August 16, 2021; accepted October 01, 2021

Abstract: Methotrexate (MTX) is widely used for the treatment of various types of cancer; however, it has drawbacks such as low solubility, lack of selectivity, premature degradation, and side effects. To solve these weaknesses, a hydrogel with the ability to contain and release MTX under physiological conditions without burst release was synthesized. The hydrogel was fabricated with a poly(ε-caprolactone)-*b*-poly(ethylene glycol)-*b*-poly(ε-caprolactone) (PCL–PEG–PCL) triblock copolymer, synthesized by ring-opening polymerization. The characterizations by proton nuclear magnetic resonance spectroscopy and Fourier-transform infrared spectrometry confirmed the copolymer assembly, whereas the molecular weight analysis validated the PCL_{2000}–PEG_{1000}–PCL_{2000} structure. The copolymer aqueous solution exhibited sol–gel phase transition at 37°C and injection capacity. The hydrogel supported a load of 1,000 μg MTX·mL^{-1}, showing a gradual and sustained release profile of the drug for 14 days, with a delivery up to 92% at pH 6.7. The cytotoxicity of the MTX-loaded hydrogel was performed by the methyl thiazole tetrazolium assay, showing a mean inhibitory concentration of 50% of MCF-7 cells (IC_{50}) at 43 μg MTX·mL^{-1}.

Keywords: copolymer, cytotoxicity, drug delivery, hydrogel, methotrexate

1 Introduction

Breast cancer is a type of metastatic cancer that is commonly resistant to chemotherapy (1,2). Methotrexate (MTX; hydrophobic in nature) is widely used as an important chemotherapeutic agent to treat this sickness. However, MTX is also used for treating other human malignancies, such as acute lymphoblastic leukemia, malignant lymphoma, osteosarcoma, breast cancer, head and neck cancer, lung cancer, choriocarcinoma, and related trophoblastic tumors (3). Unfortunately, MTX has some undesirable side effects, including depression, nausea, and anaplasia, associated with its low solubility and nonspecific action that requires high daily doses for extended periods (4), as well as its short plasma half-life of only 7 h. Despite these drawbacks, MTX is still a common drug for breast cancer treatment due to its relatively low cost.

Polymeric hydrogels are materials whose hydrophilic structure enables them to hold large amount of water in their three-dimensional systems (5). These polymeric networks can absorb biological fluids and retain their distinctive three-dimensional structure (6). In recent decades, significant advances occurred in the field of hydrogels as functional biomaterials (7), and because of their ability to embed pharmaceutical agents, they are promising materials for controlled drug release and tissue engineering (8,9).

Hydrogels have great versatility in terms of composition and ability to adjust to various routes of administration, from parenteral (e.g., intramuscular, intradermal) to nonparenteral (e.g., oral, topical) (10). Poly(caprolactone)-*b*-poly(ethylene glycol)-*b*-poly(caprolactone) (PCL–PEG–PCL) hydrogels have been widely evaluated as reservoirs for controlled drug release (11). Triblock synthesis is

* **Corresponding author: Antonia Luna-Velasco,** Department of Environment and Energy, Centro de Investigación en Materiales Avanzados, S.C. Miguel de Cervantes No. 120, Complejo Industrial Chihuahua, C.P. 31136, Chihuahua, Chih, Mexico, e-mail: antonia.luna@cimav.edu.mx, tel: +52-614-439-4864
* **Corresponding author: Erasto Armando Zaragoza-Contreras,** Department of Engineering and Materials Chemistry, Centro de Investigación en Materiales Avanzados, S.C. Miguel de Cervantes No. 120, Complejo Industrial Chihuahua, C.P. 31136, Chihuahua, Chih, Mexico, e-mail: armando.zaragoza@cimav.edu.mx, tel: +52-614-439-4811
Teresa Darlen Carrillo-Castillo: Department of Engineering and Materials Chemistry, Centro de Investigación en Materiales Avanzados, S.C. Miguel de Cervantes No. 120, Complejo Industrial Chihuahua, C.P. 31136, Chihuahua, Chih, Mexico
Javier Servando Castro-Carmona: Engineering in Design and Agricultural/Food Automation, Universidad Autónoma de Ciudad Juárez, Manuel Díaz H. No. 518-B Zona Pronaf Condominio, C.P. 32315, Ciudad Juárez, Chih, Mexico

performed by ring opening of ε-caprolactone initiated by the hydroxyl groups at the extremities of a PEG prepolymer in the presence of a catalyst (12). The conformation of this triblock allows a micellar structure that increases the solubility and distribution of drugs due to its hydrophilic shell and hydrophobic core. The PCL–PEG–PCL triblock also has thermosensitive properties between 34°C and 40°C (12). Its phase changes in response to the temperature variation have pointed this as a very useful material for biomedicine. Alami-Milani et al. performed extensive research to encapsulate dexamethasone in a triblock PCL–PEG–PCL for intraocular use (13). The loading of diclofenac in a PCL_{1000}–PEG_{2000}–PCL_{1000} thermosensitive hydrogel was reported by Patel et al. (14), finding that the hydrogel achieved a sustained drug release within 14 days. In another study, MTX was loaded in a PCL_{1250}–PEG_{1500}–PCL_{1250} hydrogel for arthritis treatment, showing controlled drug release for 14 days with a release of 74.0% of the drug at pH 7.4 (15).

Studies aimed at the release of MTX through hydrogels have reported that the low affinity of hydrogels with hydrophobic drugs is a disadvantage for drug delivery as the drug is released abruptly when exposed to a physiological environment. Thus, hydrogels are considered inefficient for hydrophobic drugs (16). To overcome this drawback, recent studies have been directed to include particles in hydrogels to provide greater affinity with hydrophobic drugs and delay their release. For instance, carbon nanotubes were included in hydrogels of chitosan/β-glycerophosphate, prolonging the release for up to 7 days although the authors did not report the concentration of MTX loaded and released (17). Also, double-component hydrogels composed of chitosan microspheres into chitosan/β-glycerophosphate hydrogels were reported with a maximum release of 76% of MTX in 41 h (18). Furthermore, gold nanoparticles were loaded into a PEG-based hydrogel, which allowed an MTX release of only 40% in 7 days, contrasting with the pristine hydrogel, which released 90% of the drug in 6 days (19).

The lack of hydrophobic blocks in hydrogels is the cause for the uncontrolled and short time release of hydrophobic drugs, as MTX. Based on the interesting results of the PCL–PEG–PCL triblocks for drug delivery, we designed a PCL–PEG–PCL triblock with hydrophobic blocks for allowing its interaction with MTX, so that it can be loaded within the hydrogel and retained for extended time. Thus, its release is not with significant bursting, and the extended retention time allows drug release in therapeutic concentrations for breast cancer treatment. The hydrogel could be applied at a specific site using the copolymer phase and release response to human body temperature (37°C) and tumor pH (6.7), respectively. The properties indicated for PCL–PEG–PCL triblock with hydrophobic blocks make it a potential material for biomedical applications to charge and release hydrophobic drugs, with the possible reduction of undesirable side effects and multiple applications.

2 Materials and methods

2.1 Materials

PEG-diol (1,000 g·mol^{-1}) was obtained from Merck (NJ, USA), whereas ε-caprolactone (99% purity) was supplied by Alfa Aesar. MTX (99% purity), tin(II)-ethylhexanoate ($Sn(Oct)_2$), dichloromethane, and petroleum ether were delivered by Sigma-Aldrich (MO, USA) and used as received.

2.2 Synthesis of PCL–PEG–PCL copolymer

The copolymer was synthesized by ring-opening polymerization (ROP), using PEG-diol as the initiator block and $Sn(Oct)_2$ as the catalyst (20,21). Approximately 10 mL (0.175 mol) of ε-CL and 5 g (0.01 mol) of PEG-diol were deposited in a three-neck reactor. The mixture was gently stirred with a magnetic bar and heated to 130°C; afterward, 0.15 g of $Sn(Oct)_2$ was added. The polymerization was kept under gentle magnetic stirring at 130°C for 6 h. Upon completion of the polymerization, the product was degassed under vacuum for 30 min, and then allowed to cool to room temperature. Next, the copolymer was dissolved in dichloromethane and filtered. The filtrate was precipitated with cold petroleum ether and finally, the solid was kept under ambient conditions for 3 days to evaporate the solvent. A white, solid, granular product was obtained with a yield of 78%, according to Eq. 1:

$$\%\ \text{Yield} = \frac{W_i}{W_o} \times 100 \tag{1}$$

where W_o and W_i stand for the monomer initial weight and copolymer weight after the purification process, respectively.

The purified copolymer was stored in airtight jars until use and analyzed by a Fourier-transform infrared spectrometry (FT-IR), proton nuclear magnetic resonance spectroscopy, differential scanning calorimetry (DSC), and gas permeation chromatography (GPC) to characterize the chemical structure, thermal behavior, and molecular weight, respectively.

2.3 Triblock molecular weight

The molecular weight of the PCL–PEG–PCL triblock was analyzed using a gel permeation chromatography equipment

(1260 Infinity GPC, Agilent, CA, USA) with a refractive index detector and a PLgel 5 μm MIXED-D column of 300 mm × 7.5 mm. The polymer was dissolved in 5 mL of tetrahydrofuran high-performance liquid chromatography grade (Fisher Scientific, NH, USA) at 40°C and then 50 μL was injected at a flow rate of 1.0 mL·min^{-1}.

2.4 Chemical structure characterization

The structure of the PCL–PEG–PCL triblock copolymer was identified by proton nuclear magnetic resonance spectroscopy (^{1}H NMR) using deuterated chloroform as the solvent and tetramethylsilane as the internal reference, at 90 MHz (Eft-90 NMR, Anasazi Instruments). In addition, the functional groups were analyzed with an FT-IR (Affinity 1S, Shimadzu), in reflectance mode with the help of a Quest ATR accessory (Specac Ltd, United Kingdom), using a one-step diamond window. Each spectrum has a resolution of 4 cm^{-1} and is the average of 45 scans.

2.5 Sol–gel transition

The sol–gel transition was determined using the inverted tube method (21–23). In 4 mL vials (1 cm in diameter), amount of the copolymer was deposited to obtain systems from 10 to 50 wt% (100, 200, 300, 400, and 500 mg) in 1 mL distilled water. All vials were immersed in a water bath at 60°C for 5 min to dissolve the copolymer, and then the vials were transferred to an ice bath for 1 min and, later, immersed in another bath at 27°C for 10 min. For the gel transition, the samples in the sol state were immersed in the water bath at 27°C, and the temperature was progressively increased by 2°C until reaching 52°C. The vials were kept at each temperature for 2 min and then inverted to observe whether or not the gel was formed, which was manifested by the total absorption of water by the copolymer. In the sol state, the sample was classified as "flowing," whereas on the contrary, it was classified as "not flowing."

2.6 Aqueous solution temperature sweep

The copolymer phase transition in the sol state was characterized using a rotational rheometer (MCR-501, Anton Paar Physica) with concentric cylinder geometry. Temperature sweep tests were performed from 5°C to 60°C at a ramp rate of 2°C·min^{-1}, 1 Hz, and deformation of 0.01%.

2.7 *In situ* hydrogel formation

To confirm the *in situ* hydrogel formation, solutions were prepared at 27°C with 20 wt% copolymer. To 1 mL of the solution, 0.01 mg of methyl red dye was added to visualize the gel in an aqueous environment. The colored solution was loaded at room temperature into a hypodermic syringe with a 21G needle (Plastipak, MI, USA) and then injected into a vial containing water at 37°C. For comparison purposes, an aqueous solution of methylene red (0.01 mg·mL^{-1}) was also injected into a vial with water under the same conditions.

2.8 Aqueous solution injectability

A cucumber (*Cucumis sativus*) was used to evaluate the injectability of the copolymer solution at room temperature. For this, a section of 5 cm cross-section and 1.0 cm × 0.5 cm rectangle was drilled on the vegetable surface. The vegetable portion was tempered in a water bath at 37°C for 20 min. Afterward, 1.0 mL of the solution with 20 wt% copolymer was loaded into a 3 mL hypodermic syringe with a 21G needle. The solution was then injected into the vegetable and deposited in the drilled area.

2.9 Morphology characterization

The hydrogel morphology was evaluated using a field-emission scanning electron microscope (JSM 7401F, JEOL). To prepare the sample, the hydrogel was frozen with liquid nitrogen, followed by lyophilization (Freezone 6, Labconcoat) at −40°C and a vacuum pressure of 3,000 Pa for 24 h.

2.10 Loading of MTX and release assay

To load the MTX into the hydrogel, a 10 mL copolymer aqueous solution at 20 wt/vol% was prepared. Then, 1 mL of this solution and 1 mg of MTX were added and thoroughly mixed in a vial until homogenization. The fluid solution was brought to its gel state immersing the vial in a water bath at 37°C for 3 min, thus leaving the hydrogel loaded with 1,000 μg·mL^{-1} of MTX, which was designated as MTX-H. For the drug-release assay, 10 mL of phosphate-buffered saline (PBS) at pH 7.4 and 6.7 was poured in vials with MTX-H. The former simulates the normal condition of the human body, whereas the latter simulates the environment of a tumor. The vials were placed in a temperature-controlled chamber (LSE Benchtop, Corning),

keeping gentle stirring (60 rpm) and 37°C. Each time, 2 mL of PBS was collected from each vial and the same amount of fresh PBS (preheated to 37°C) was added. The amount of MTX released was determined by UV-Vis spectroscopy at 303 nm, which was expressed as a cumulative percentage of the released drug (Cr) using Eq. 2 (24):

$$\text{Cr}\ (\%) = \frac{V_t \sum_1^{n-1} C_i + V_0 C_n}{m_{\text{MTX}}} \times 100 \quad (2)$$

where m_{MTX} is the amount of MTX in the hydrogel, V_0 is the total volume of PBS used for the release (V_0 = 10 mL), V_t is the volume of the replaced PBS (V_t = 2 mL), and C_n represents the concentration of MTX in the sample.

2.11 Cytotoxicity of MTX-H on MCF-7 cells

The cytotoxicity of MTX, MTX-H, and PCL–PEG–PCL was evaluated in the human breast cancer cell line MCF-7 ATCC® HTB-22™, using the methyl thiazole tetrazolium (MTT) assay. The cells were cultured in a dulbecco's modified eagle medium supplemented with 10% fetal bovine serum and incubated at 37°C in a 90% humidified environment and 5% CO_2/95% air. The medium was replaced every 24–48 h, until reaching a cellular confluence of 80–90% required to perform the tests.

MCF-7 cells were extracted from the culture dishes and seeded in 96-well microplates at a cell density of 1×10^4 cells/well with 200 µL of culture media and incubated for 24 h for adhesion. Next, the old culture medium was discarded and a new culture medium was added to the cell monolayer. Then, an adequate volume of stock solutions of MTX, MTX/PCL-PEG-PCL, or PCL-PEG-PCL was added in the medium to obtain the MTX concentrations of 10, 20, 30, 60, and 90 µg mL^{-1}, and the respective concentrations of the copolymer of 2, 4, 6, 12, and 18 mg mL^{-1}. The microplate was incubated for 72 h under the same culture conditions. Positive and negative control samples were included. All treatments and controls were carried out in triplicate.

After incubation, the MTT test was performed. All media having drug and/or copolymer were removed from wells, and cells were once gently washed with PBS at pH 7.4. Subsequently, 180 µL of culture medium and 20 µL of MTT (50 µg·mL^{-1}) were added to each well, and the microplate was incubated for another 4 h. Then, the media were removed, and 200 µL of acidified isopropanol was added to each well to dissolve the cell-metabolized formazan. The absorbance of each well was measured at 570 nm using a microplate reader (Varioskan LUX, Thermo Fisher Scientific, MA, USA). Cell viability, relative to untreated cells (control), was determined by Eq. 3:

$$\text{Cell viability}\ (\%) = \frac{\text{OD}_{(\text{Test})}}{\text{OD}_{(\text{Reference})}} \times 100 \quad (3)$$

where $\text{OD}_{(\text{Test})}$ and $\text{OD}_{(\text{Reference})}$ represent the mean absorbance of the treated cells and the absorbance of the reference cells, respectively.

3 Results and discussion

3.1 Copolymer characterization

The copolymer was synthesized by ROP, using PEG-diol as the initiating block and $Sn(Oct)_2$ as the catalyst (20,21). The copolymer was synthesized through a direct catalytic-type mechanism, where the catalyst activates the monomer by coordination with its carbonyl oxygen. The polymerization mechanism is well known and previously reported (25).

Figure 1 shows the FT-IR copolymer spectrum, stretching vibration of the terminal hydroxyl group is observed at 3,523 cm^{-1}; whereas the vibrations of the symmetric and asymmetric stretching of the C–H bonds of the methylene groups appear at 2,948 and 2,859 cm^{-1}, respectively. Symmetric stretching of the C═O carbonyl group of PCL appears at 1,722 cm^{-1}, and the stretching vibration of C–O is observed at 1,370 cm^{-1}. The peak at 1,099 cm^{-1} corresponds to the stretching of the C–O–C group of PEG, but it was also associated with the formation of the ester group that binds the blocks. Finally, the vibration at 726 cm^{-1} corresponds to the alkyl radicals, evidencing ring opening. As noted, this spectrum matches the signals reported for equivalent copolymers (20,21).

Figure 2 shows the ^{1}H NMR spectrum for copolymers. As noted, the prominent signal at 3.6 ppm corresponds to protons (a) and (b) of the methyl ether of PEG (13), whereas signal at 2.29 ppm shows the protons neighboring the carbonyl of the PCL (c) $-CH_2CO-$, whereas the signals 1.48, 1.63, and 1.71 ppm represent the methylene protons derived from the opening of the PCL ring (d–f) $-(CH_2)-$ (26). Next, the signal at 4.10 ppm shows the protons that bind to the PCL units (g) (27). Finally, the signal at 3.14 ppm is attributed to the methylene protons where the end of the PEG block was linked to the PCL block (21).

3.2 Molecular weight analysis

The molecular weight of the copolymer was established by GPC. The molecular weight at the maximum peak (M_p),

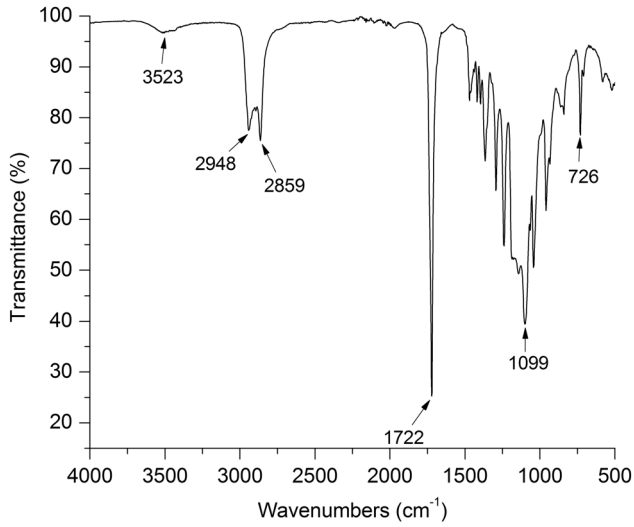

Figure 1: FT-IR spectrum of PCL–PEG–PCL copolymer.

number average molecular weight (M_n), and molecular dispersity index were 6,280 g·mol^{-1}, 5,090 g·mol^{-1}, and 1.27, respectively. Since the M_n of the PEG block is 1,000 g·mol^{-1}, the difference of 4,090 g·mol^{-1} is attributed to the PCL blocks. If it is considered that the polymerization proceeds with the same probability and speed at both ends of the central block, then the molecular weight value obtained by GPC can be divided between the two PCL blocks, obtaining a triblock structure PCL_{2000}–PEG_{1000}–PCL_{2000}. It has been reported that for the sol-to-gel transition, the PCL block must be larger than the PEG block because it provides stability and phase changes at defined temperatures (27). It was also reported that when the length of the PCL chain is longer, the hydrophobic PCL segments can be packed more efficiently, and hydrophobic interactions within the core of the micelles increase. This favors the self-assembly of PCL–PEG–PCL copolymers in aqueous solutions at low levels and could keep the drug encapsulated. This micellar stability prevents dissociation and undirected the drug release (26).

3.3 Thermal characterization

Figure 3 shows the DSC trace of the copolymer. As noted, the cooling process exhibits two exothermic transitions, one at –2.4°C, attributed to the crystallization of PEG, and the other at 17.42°C, ascribed to PCL crystallization (28).

During the heating process, a melting peak was observed at 27.4°C, associated with the melting of the PEG segment. In addition, two melting peaks are shown, one at 40.7°C and the other at 47.3°C, assigned to the melting of the PCL segment and the melting of the recrystallized PCL domain during the heating process, respectively (28). Gong et al. synthesized a chemical-configured triblock copolymer PCL_{2000}–PEG_{1000}–PCL_{2000}. They reported that the copolymer cooling process showed two exothermic transitions, at –2°C and 20°C, ascribed to the crystallization of PEG and PCL, respectively. During the heating process, they observed a melting peak at 25°C that was assigned to the melting of the PEG segment. In addition, they also reported endothermic peaks at 41°C and 50°C, corresponding to the fusion of the PCL segment, followed by the fusion of the recrystallized PCL domain during the heating process (29).

3.4 Sol–gel transition

The inverted tube method (21–23) was used to determine the concentration at which the copolymer changes from

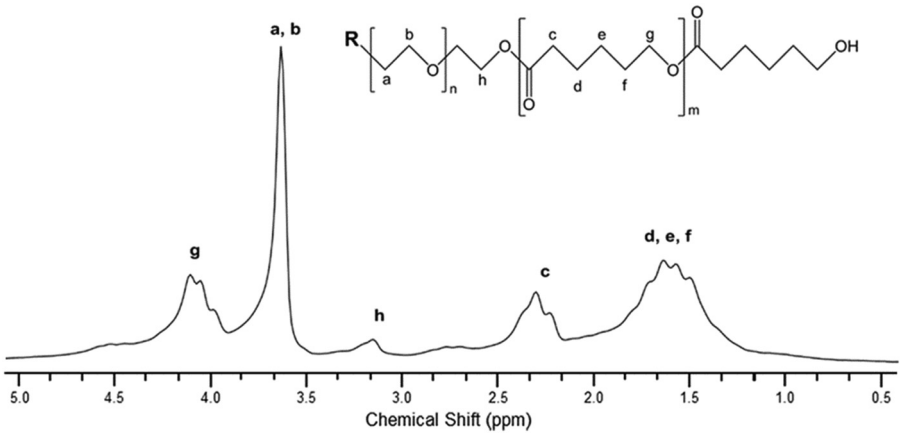

Figure 2: ^{1}H NMR spectrum of the PCL–PEG–PCL triblock copolymer.

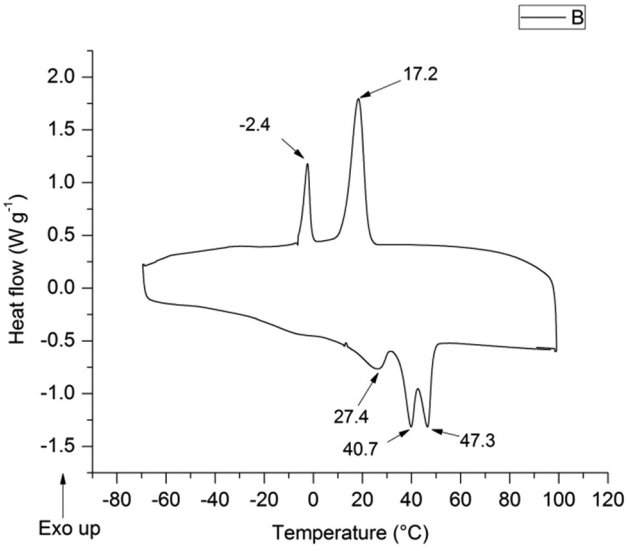

Figure 3: DSC traces of PCL–PEG–PCL copolymer.

the fluid state to the hydrogel state when the temperature approaches 37°C (body temperature; Figure 4).

For this, solutions at 10, 20, 30, 40, and 50 wt% copolymer in 1 mL of water were tested. First, the systems were heated to 60°C; at this temperature, all the systems were fluid. Subsequently, the containers were transferred to an ice bath so that the sudden cooling prevented hydrogel formation since a slow cooling would cause the gel formation when the solution passed through the copolymer phase change temperature, from 60°C to 37°C. At the ice bath temperature, all the solutions remained in fluid state. Subsequently, to determine whether a system remained in the sol state at room temperature, the vials were immersed in a bath at 27°C. Finally, to determine sol-to-gel transition, a temperature ramp of 2°C was applied. In this last step, the phase transition at 37°C (36.5°C) was considered for the rest of experimentation because this is commonly reported as body temperature.

Under previous considerations, the following was observed: (1) the 10 wt% copolymer solution remained fluid until 5°C showing no phase change; (2) for the 20 and 30 wt% copolymer solutions, sol-to-gel transition occurs at 37°C, remaining solid up to 41°C, but by continuing to increase the temperature, the hydrogels returned to the fluid state; and (3) finally, for 40 and 50 wt% copolymer systems, the phase change shows at 33°C and 29°C, respectively, being unsuitable for a drug-delivery system. Based on these results, it was determined that the content of 20 wt% copolymer is the appropriate to load and release drugs and nanoparticles. Ma et al. also reported that the 20 wt% content of their copolymer presented a phase change at physiological temperature (27). Vaishya commented that the copolymer does not spontaneously form micelles in an aqueous solution, but the crystallinity of PCL prevents the polymer from spontaneously self-assembling. Therefore, it is necessary to heat the polymer to its melting point to give the PCL fragments the necessary mobility and make it possible for the polymer to self-assemble, forming the micelle (30). Therefore, according to the DSC data, the aqueous copolymer dispersions were heated to 60°C, a temperature above the melting point of the copolymer, corresponding to the PCL fragment, followed by rapid cooling in an ice bath, and thus, it was achieved that the copolymer self-assembled into micelles.

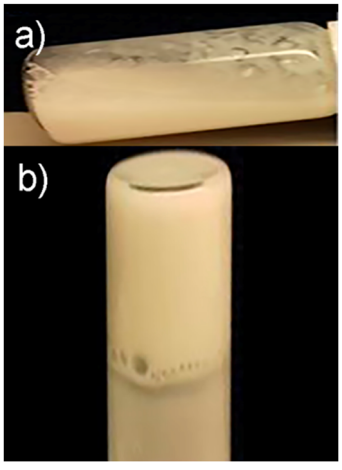

Figure 4: PCL–PEG–PCL triblock copolymer (20 wt%) in the sol state at 27°C (a) and in the gel state at 37°C (b).

3.5 Temperature sweep of the aqueous solution

The gelling mechanism of a thermosensitive physical hydrogel is explained by the packing of micelles motivated by hydrophobic interactions and the partial crystallization of the PCL blocks as soon as the temperature increases (21), which begins to dissolve the micelles causing their swelling. Aqueous PCL–PEG–PCL solutions spontaneously transform into hydrogel above a critical gel concentration around body temperature. When the triblock copolymer is fully dispersed and dissolved in water, the hydrophobic block of PCL and the hydrophilic block of PEG self-assemble to form micelles, which move freely in the aqueous solution (31). The PEG block loops out of the micelle while it swells with increasing temperature, and when close enough to another block of

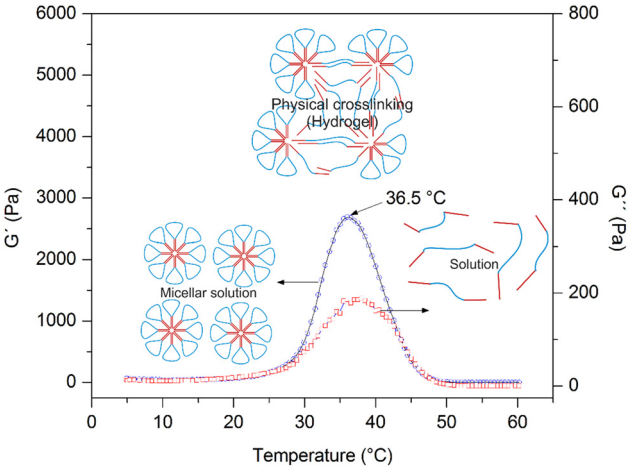

Figure 5: Temperature sweep of the PCL–PEG–PCL copolymer in aqueous phase. The sol–gel transition occurs at 36.5°C.

neighboring micelles, they form a bridge motivated by noncovalent molecular attractions that result in the formation of big particles in the system (32).

In the temperature sweep (Figure 5), it was observed that below 5°C the crossing point between the storage modulus (G') and the loss modulus (G'') appears, indicating that at this point, micellar structure association begins (31). As the temperature increases, G' was located above G'', which indicates a micellar association, creating a associated network, favored by the hydrophobic PCL moieties and hydrogen bonding (32). By continuing to increase the temperature, the micellar association decreases, reaching complete dissociation at 50°C, where the two modules approach, revealing that the polymer becomes soluble; consequently, the micellar association no longer exists.

Studies focused on different lengths of the PCL blocks have reported that when the block is longer than the length of the hydrophilic PEG block, an increase of micellar stability arises (27). So, the micellar structure with a longer PCL block is expected to be more stable and will break at higher temperatures. In addition to the effects of chemical composition, the copolymer content also showed a significant influence on sol–gel transition, as the phase-transition temperature increases. This change influenced by temperature is the desired behavior for a drug-delivery system (27,29).

3.6 Gel formation

To confirm the *in situ* gel formation of PCL_{2000}–PEG_{1000}–PCL_{2000}, solutions of the copolymer were prepared. The incorporation of the methyl red dye was intended to allow visualizing the hydrogel dynamics when injected into a water mass. This test shows the behavior of the copolymer solution when comes in contact with an environment at a similar temperature to that of the human body. When the colored fluid solution of the copolymer was injected into the water mass at 37°C, the formation of the hydrogel was immediately observed, heading to the vial's bottom, where it remained undissolved (Figure 6a). In contrast, when the methyl red aqueous solution was injected under the same conditions, it diffused freely in the water bulk, without a defined pattern, remaining that way at all times (Figure 6b). Equivalent behaviors were reported by Ma et al., stating that the aqueous solutions of their PCL_{1250}–PEG_{1500}–PCL_{1250} copolymer instantly formed a gel after injection, whereas the aqueous solution of red dye spontaneously diffused into the water (27).

To corroborate the temperature influence on the copolymer phase change, the colored solution was injected in a vial with water at room temperature. As expected, the phase change was not observed, the fluid solution with the dye diffused freely into the water, revealing the dissolution of both the dye and copolymer. To delve more deeply into the temperature effect, the rheological behavior at 45°C was considered (Figure 5), where a second phase change occurred. Thus, the copolymer solution was injected into another vial with water at 45°C. At that temperature, there was no hydrogel formation, again observing the free diffusion of the dye in the water bulk. The nonwater soluble, methyl red indicator, exemplifies the expected behavior of the drug being loaded in the hydrogel when exposed to different temperatures. Therefore, this test shows that the obtained hydrogel is able to capture the drug at physiological temperature.

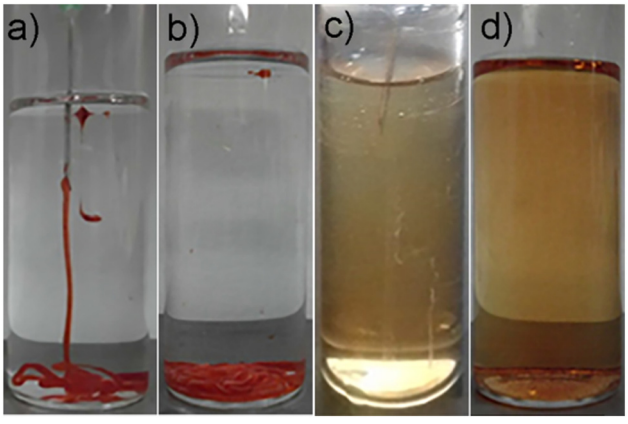

Figure 6: Hydrogel formation when injected in water at 37°C (a and b). Methyl red solution when injected under the same conditions (c and d).

To provide more evidence about both the copolymer injectability in the sol state and hydrogel formation at 37°C, 1.0 mL of the aqueous solution was injected into a portion of cucumber (*C. sativus*) previously tempered to 37°C. As noted, the solution flowed freely throughout the needle and settled into the cavity pierced in the vegetable. After 1 min, the white hydrogel is formed, remaining in that form even after the vegetable temperature dropped to 27°C (Figure 7).

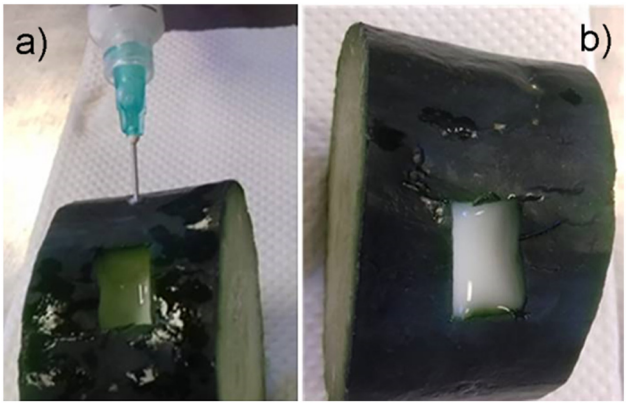

Figure 7: Injectability of the hydrogel into a section of a cucumber (*C. sativus*) preheated to 37°C. (a) Injection of the triblock solution at laboratory temperature, and (b) the hydrogel is formed after reaching 37°C of the cucumber surface.

3.7 Hydrogel morphology

The hydrogel formed with 20 wt% copolymer was frozen with liquid nitrogen and lyophilized for 24 h. The solid obtained was analyzed by scanning electron microscopy (Figure 8); the micrograph shows a porous three-dimensional structure of a homogeneous size typical of a hydrogel. The hydrogel pores were formed when the network structure captured the water in the hydrophilic blocks. The average pore size is about 5 μm, so it is expected that the drug molecules can lodge in the pores; accordingly, the system promises to be suitable for use as a delivery system.

3.8 Loading and releasing of MTX

The amount of MTX released was determined by UV-Vis spectroscopy at 303 nm, which was expressed as a cumulative percentage of the released drug (Cr) base on time. Figure 9 illustrates the release behavior of MTX from the hydrogel. As observed, both systems present an initial acute release profile during the first two days, with a greater release in the acidic environment, which reached up to 35% release, whereas at neutral pH, 25% was released at the same time. After the second day, the system of pH 7.4 no longer showed greater release, keeping in equilibrium during the 20 days. Differently, the hydrogel at pH 6.7 shows a gradual and sustained release until day 14 when its maximum accumulated release was 92%. After that time, it remained in equilibrium until day 20. The initial acute release of the two systems is attributed to the superficial drug contained in the hydrogel, and the gradual drug release was related to that which was trapped in the polymeric network when the copolymer changed from the fluid to the gel state. It is worth noting that the acidic pH influences the system release, causing the network to swell, allowing the drug to release. However, at neutral pH, in which the network does not swell, the drug is not released. Considering that drug release from hydrogels is the combined result of two processes: drug diffusion and hydrogel degradation (33), and considering that PCL is a highly hydrophobic crystalline polymer that degrades very slowly *in vitro* in the absence of enzymes (34), the 14-day period of release is not sufficient to attribute it to degradation; therefore, the diffusion process of the drug is the key factor for the release at that time.

Loading and releasing studies using PCL–PEG–PCL hydrogels have shown comparable patterns; for example, Patel et al. used a PCL_{1000}–PEG_{2000}–PCL_{1000} thermosensitive hydrogel to load sodium diclofenac, and the results indicated that the hydrogel achieved a sustained release of 90% over a period of 14 days, showing a rate reduction after 10 days (14). Also, Miao et al. reported that the

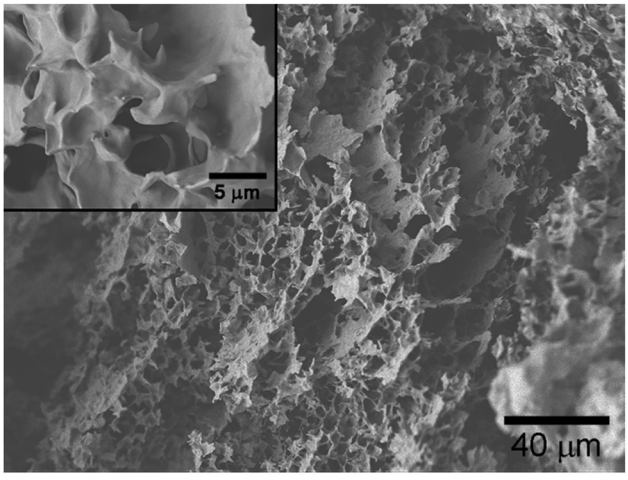

Figure 8: Micrograph of the PCL–PEG–PCL hydrogel.

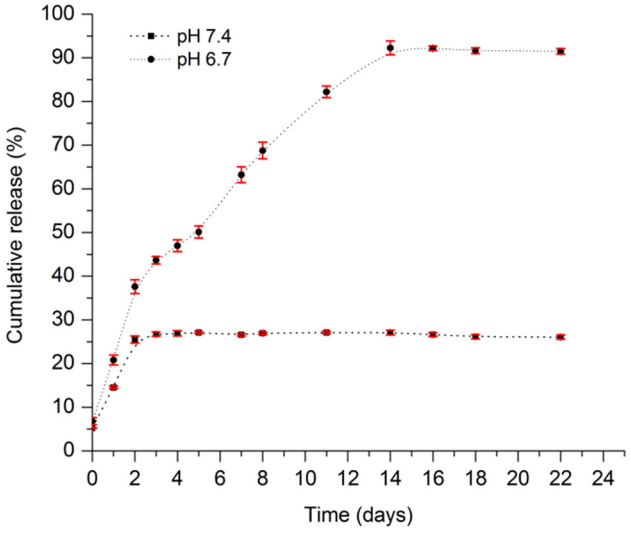

Figure 9: Percentage of cumulative release of MTX from the H/MTX system in PBS at pH 7.4 and 6.7, for 22 days.

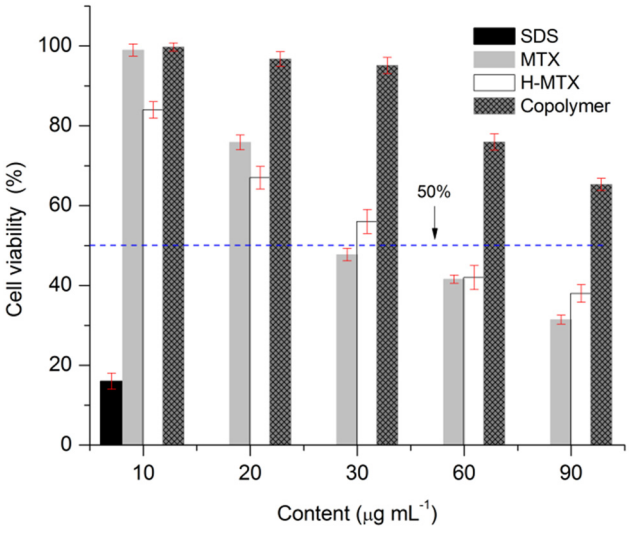

Figure 10: Cytotoxic effect of the free drug MTX, MTX/PCL–PEG–PCL, and PCL–PEG–PCL on MCF-7 cells, determined by MTT assay at 72 h of incubation. Data are presented as mean ± SD.

cumulative release rate of MTX decreased with increasing drug load, and that a higher concentration of hydrogel resulted in a more condensed structure, reducing the rate of drug diffusion, which led to a lower cumulative release rate (15).

3.9 Cytotoxicity of MTX-H in MCF-7 cells

The cytotoxic effect of free MTX, MTX-H, and copolymer was evaluated using the MTT assay. Cells treated with sodium dodecyl sulfate (0.1%) were included as a reference for reduced viability and untreated cells as a positive control (100% viability). The regression equation ($y = 4 \times 10^{-5}x + 0.3452$; $R^2 = 0.9635$) obtained from a lineal cell curve was used to estimate the viable cells in assay. Then the percentage of viability on each treatment was obtained by applying Eq. 3. Each treatment was performed in triplicate.

The cell viability for the free MTX, MTX-H system, and PCL–PEG–PCL copolymer is shown in Figure 10. The MTX concentrations evaluated for both free MTX and MTX contained in the hydrogel were 10, 20, 30, 60, and 90 μg·mL^{-1}. The equivalent copolymer concentrations of 2, 4, 6, 12, and 18 mg·mL^{-1} were also assayed.

A cell viability of 100% was observed at the lowest concentration of free MTX, and as the concentration increases, the viability decreases, reaching 30% at 90 μg·mL^{-1}. The mean inhibitory concentration of 50% (IC_{50}) calculated was of 43 μg·mL^{-1}. As for MTX-H, at the lowest concentration of the drug, the cell viability was decreased to 82%, and the viability also decreased as the drug concentration increased, obtaining an IC_{50} of 30 μg MTX·mL^{-1}. The cytotoxicity of the MTX-H is attributed to the drug contained in the hydrogel since the equivalent amount of copolymer (6 mg·mL^{-1}) allowed a cell viability of almost 100%. At the higher dose of copolymer (18 mg·mL^{-1}), the cell viability was of 70%; thus, the PCL_{2000}–PEG_{1000}–PCL_{2000} is considered noncytotoxic at these concentrations.

A recent study, in which MTX was conjugated to polymer quantum dots, reported an IC_{50} of 25 μg·mL^{-1} in MCF-7 cells (35), a value close to the IC_{50} of 30 μg·mL^{-1} presented by MTX-H. Furthermore, Gou et al. reported that a PCL–PEG–PCL triblock copolymer was noncytotoxic up to 5 mg·mL^{-1} (62% viability), whereas our copolymer presented that cytotoxicity up to 18 mg·mL^{-1}. The higher cytotoxicity of that copolymer is related to its high molar mass (17,000 g·mol^{-1}), compared to the lower value (5,090 g·mol^{-1}) of the copolymer used in this work (36). According to the results, it is concluded that the MTX-H can achieve a cytotoxic effect up to 40% viability for the MCF-7 cell line in a time of 72 h, with a copolymer content whose cytotoxicity remains lower than the IC_{50}.

4 Conclusion

The synthesis by ROP allowed us to obtain a PCL–PEG–PCL triblock copolymer that presents a change in the sol-to-gel phase of a physical type dependent on the concentration and the temperature. The sol state is injectable at

room temperature, turning into the gel state *in situ* at 37°C (human body temperature). The hydrogel shows a three-dimensional structure with interconnected pores of a suitable size to house the MTX. The hydrogel in the sol state could capture MTX, switching to the gel state and subsequently releasing it in a simulated physiological environment stimulated by an acidic pH. Furthermore, most of the drug remained encapsulated in a neutral physiological environment. As the fluid form of the gel, it can be injected at the specific site of the tumor. Also, it could prevent secondary reactions because with a single application, the loaded MTX can be released for 14 days at concentration with a cytotoxic effect on cancer cells. Finally, the hydrogel loading capacity represents a promising quality for breast cancer treatments.

Acknowledgment: We thank the Laboratorio Nacional de Nanotecnología (CIMAV) and Erika López, Claudia Hernández, and Karla Campos for their valuable support during the development of this project.

Funding information: This project was funded by the National Council for Science and Technology of Mexico (CONACYT) through the Project CB 2014-241001 and with the scholarship awarded to Teresa Darlen Carrillo-Castillo (447478).

Author contributions: Teresa Darlen Carrillo-Castillo: investigation, writing – original draft, methodology, formal analysis; Antonia Luna-Velasco: resources, supervision, formal analysis, visualization, writing – review and editing; Erasto Armando Zaragoza-Contreras: formal analysis, resources, supervision, visualization, writing – review and editing; and Javier Servando Castro-Carmona: conceptualization, funding acquisition, resources, and supervision.

Conflict of interest: Authors state no conflict of interest.

References

(1) Abad E, García-Mayea Y, Mir C, Sebastian D, Zorzano A, Potesil D, et al. Common metabolic pathways implicated in resistance to chemotherapy point to a key mitochondrial role in breast cancer. Mol Cell Proteomics. 2019;18:231–44. doi: 10.1074/mcp.RA118.001102.

(2) Lehuédé C, Li X, Dauvillier S, Vaysse C, Franchet C, Clement E, et al. Adipocytes promote breast cancer resistance to chemotherapy, a process amplified by obesity: Role of the major vault protein (MVP). Breast Cancer Res. 2019;21:1–17. doi: 10.1186/s13058-018-1088-6.

(3) Yoon S-A, Choi JR, Kim J-O, Shin J-Y, Zhang X, Kang J-H. Influence of reduced folate carrier and dihydrofolate reductase genes on methotrexate-induced cytotoxicity. Cancer Res Treat. 2010;42:163. doi: 10.4143/crt.2010.42.3.163.

(4) Manish G, Vimukta S. Targeted drug delivery system: a review. Res J Chem Sci. 2011;1:135–8.

(5) Ahmed EM. Hydrogel: Preparation, characterization, and applications: a review. J Adv Res. 2015;6:105–21.

(6) Vlierberghe S, Van, Dubruel P, Schacht E. Biopolymer-based hydrogels as scaffolds for tissue engineering applications: a review. Biomacromolecules. 2011;12:1387–1408. doi: 10.1021/bm200083n.

(7) Bakaic E, Smeets NMB, Hoare T. Injectable hydrogels based on poly(ethylene glycol) and derivatives as functional biomaterials. RSC Adv. 2015;35469–86. doi: 10.1039/c4ra13581d.

(8) Buwalda SJ, Boere KWM, Dijkstra PJ, Feijen J, Vermonden T, Hennink WE. Hydrogels in a historical perspective: from simple networks to smart materials. J Control Release. 2014;190:254–73. doi: 10.1016/j.jconrel.2014.03.052.

(9) Ullah F, Bisyrul M, Javed F, Akil H. Classification, processing and application of hydrogels: a review. Mater Sci Eng C. 2015;57:414–33. doi: 10.1016/j.msec.2015.07.053.

(10) Sosnik A, Seremeta K. Polymeric hydrogels as technology platform for drug delivery applications. Gels. 2017;3:25. doi: 10.3390/gels3030025.

(11) Steinman NY, Bentolila NY, Domb AJ. Effect of molecular weight on gelling and viscoelastic properties of poly(caprolactone)-*b*-poly(ethylene glycol)-*b*-poly(caprolactone) (PCL–PEG–PCL) hydrogels. Polymers (Basel). 2020;12:1–11.

(12) Huynh DP, Nguyen MK, Pi BS, Kim MS, Chae SY, Lee KC, et al. Functionalized injectable hydrogels for controlled insulin delivery. Biomaterials. 2008;29:2527–34. doi: 10.1016/j.biomaterials.2008.02.016.

(13) Alami-Milani M, Zakeri-Milani P, Valizadeh H, Salehi R, Jelvehgari M. Preparation and evaluation of PCL–PEG–PCL micelles as potential nanocarriers for ocular delivery of dexamethasone. Iran J Basic Med Sci. 2018;21:153–64. doi: 10.22038/ijbms.2017.26590.6513.

(14) Patel P, Mandal A, Gote V, Pal D, Mitra AK. Thermosensitive hydrogel-based drug delivery system for sustained drug release. J Polym Res. 2019;26:131. doi: 10.1007/s10965-019-1771-z.

(15) Miao B, Song C, Ma G. Injectable thermosensitive hydrogels for intra-articular delivery of methotrexate. J Appl Polym Sci. 2011;122:2139–45. doi: 10.1002/app.

(16) Dehshahri A, Kumar A, Madamsetty VS, Uzieliene I, Tavakol S, Azedi F, et al. New horizons in hydrogels for methotrexate delivery. Gels. 2021;7:1–20. doi: 10.3390/gels7010002.

(17) Saeednia L, Yao L, Cluff K, Asmatulu R. Sustained releasing of methotrexate from injectable and thermosensitive chitosan-carbon nanotube hybrid hydrogels effectively controls tumor cell growth. ACS Omega. 2019;4:4040–8. doi: 10.1021/acsomega.8b03212.

(18) Dang Q, Liu C, Wang Y, Yan J, Wan H, Fan B. Characterization and biocompatibility of injectable microspheres-loaded hydrogel for methotrexate delivery. Carbohydr Polym. 2016;136:516–26. doi: 10.1016/j.carbpol.2015.09.084.

(19) Nutan B, Chandel AKS, Biswas A, Kumar A, Yadav A, Maiti P, et al. Gold nanoparticle promoted formation and biological properties of injectable hydrogels. Biomacromolecules. 2020;21:3782–94. doi: 10.1021/acs.biomac.0c00889.

(20) Feng R, Song Z, Zhai G. Preparation and in vivo pharmacokinetics of curcumin-loaded PCL–PEG–PCL triblock copolymeric nanoparticles. Int J Nanomed. 2012;7:4089–98. doi: 10.2147/IJN.S33607.
(21) Liu CB, Gong CY, Huang MJ, Wang JW, Pan YF, Zhang Y, et al. Thermoreversible gel–sol behavior of biodegradable PCL–PEG–PCL triblock copolymer in aqueous solutions. J Biomed Mater Res B Appl Biomater. 2007;83:165–75. doi: 10.1002/jbm.b.30858.
(22) Feng Z, Zhao J, Li Y, Xu S, Zhou J, Zhang J, et al. Temperature-responsive in situ nanoparticle hydrogels based on hydrophilic pendant cyclic ether modified PEG–PCL–PEG. Biomater Sci. 2016;4:1493–502. doi: 10.1039/C6BM00408C.
(23) Ni PY, Ding QX, Fan M, Liao JF, Qian ZY, Luo JC, et al. Injectable thermosensitive PEG–PCL–PEG hydrogel/acellular bone matrix composite for bone regeneration in cranial defects. Biomaterials. 2014;35:236–48. doi: 10.1016/j.biomaterials.2013.10.016.
(24) Deng H, Liu J, Zhao X, Zhang Y, Liu J, Xu S, et al. PEG-*b*-PCL copolymer micelles with the ability of pH-controlled negative-to-positive charge reversal for intracellular delivery of doxorubicin. Biomacromolecules. 2014;15:4281–92. doi: 10.1021/bm501290t.
(25) Dechy O, Martin B, Bourissou D. Controlled ring-opening polymerization of lactide and glycolide. Chem Rev. 2004;104:6147–76. doi: 10.1021/cr040002s.
(26) Kocabay ÖG, Ismail O. Synthesis and characterization of poly (ε-caprolactone)-poly(ethylene glycol)-poly(ε-caprolactone) copolymers: investigation of the effect of blocks on micellization. Rev Roum Chim. 2018;63:1157–67.
(27) Ma G, Miao B, Song C. Thermosensitive PCL–PEG–PCL hydrogels: synthesis, characterization, and delivery of proteins. J Appl Polym Sci. 2010;116:2658–67. doi: 10.1002/app.
(28) Bae SJ, Suh JM, Sohn YS, Bae YH, Kim SW, Jeong B. Thermogelling poly(caprolactone-b-ethylene glycol-b-caprolactone) aqueous solutions. Macromolecules. 2005;38:5260–5. doi: 10.1021/ma050489m.
(29) Gong CY, Shi S, Dong PW, Yang B, Qi XR, Guo G, et al. Biodegradable in situ gel-forming controlled drug delivery system based on thermosensitive PCL–PEG–PCL hydrogel: part 1 – synthesis, characterization, and acute toxicity evaluation. J Pharm Sci. 2009;98:4684–94. doi: 10.1002/jps.21780.
(30) Vaishya RD, Gokulgandhi M, Patel S, Minocha M, Mitra AK. Novel dexamethasone-loaded nanomicelles for the intermediate and posterior segment uveitis. AAPS Pharm Sci Tech. 2014;15:1238–51. doi: 10.1208/s12249-014-0100-4.
(31) Winnik MA, Yekta A. Associative polymers in aqueous solution. Curr Opin Colloid Interface Sci. 1997;2:424–36. doi: 10.1016/s1359-0294(97)80088-x.
(32) Chassenieux C, Nicolai T, Benyahia L. Rheology of associative polymer solutions. Curr Opin Colloid Interface Sci. 2011;16:18–26. doi: 10.1016/j.cocis.2010.07.007.
(33) Gu D, O'Connor AJ, Qiao GGH, Ladewig K. Hydrogels with smart systems for delivery of hydrophobic drugs. Expert Opin Drug Deliv. 2017;14:879–95. doi: 10.1080/17425247.2017.1245290.
(34) Bromberg LE, Eyal SR. Temperature-responsive gels and thermogelling polymer matrices for protein and peptide delivery. Adv Drug Deliv Rev. 1998;31:197–221.
(35) Rafienia M, Nasirian V, Mansouri K, Vaisi-Raygani A. Methotrexate-conjugated to polymer quantum dot for cytotoxicity effect improved against MCF-7 and Hela cells. Med Chem Res. 2018;27:1578–88. doi: 10.1007/s00044-018-2173-1.
(36) Gou M, Zheng L, Peng X, Men K, Zheng X, Zeng S, et al. (PCL–PEG–PCL) nanoparticles for honokiol delivery in vitro. Int J Pharm. 2009;375:170–6. doi: 10.1016/j.ijpharm.2009.04.007.